Coherent mode decomposition of Kolmogorov optical turbulence in a finite aperture

Yousef K. Chahine*

*NASA Glenn Research Center, Cleveland, Ohio, 44135

ABSTRACT

An analysis of the coherent mode decomposition of an optical field after propagation through atmospheric turbulence is presented. The coherent modes represent an ideal basis by which to decompose the field for design of mode-limited optical systems. Due to rotational symmetry of the Fredholm integral operator for Kolmogorov optical turbulence, the coherent modes exhibit separable solutions classified by a radial and azimuthal mode index. The study of the coherent modes is then reduced to that of the radial functions determined by the coherence ratio D/r_0 and obscuration ratio ϵ. Analysis of the spectrum of eigenvalues yields sharp bounds on the efficiency of receivers using incoherent or coherent combining with mode-limited photonic devices in the presence of Kolmogorov turbulence. The effective number of modes needed to represent Kolmogorov optical turbulence is studied via the von Neumann entropy, purity, and largest eigenvalue, and the differences in the different definitions is discussed. The similarity of the coherent modes to linearly polarized (LP) fiber modes is quantified yielding a precise characterization of the maximum gain that can be achieved in mode-limited systems via mode shaping techniques. As a final application, a mode sorting technique is presented for optimally splitting power from atmospherically degraded light into a finite number of modes simultaneously maximizing total coupling efficiency and minimizing the difference in average power between channels.

Keywords: free-space optical communication, atmospheric turbulence, coherence and statistical optics, coherent mode decomposition

1. INTRODUCTION

In this work, we are interested in understanding the spatial mode structure of a laser beam arriving at a finite-aperture receiver after propagation through an atmospheric free-space optical channel. In particular, we are interested in a precise characterization of the degradation of a pure optical mode at the transmitter into some ensemble of spatial modes which are received at the aperture with and without low-order correction in the form of tilt compensation with a fast steering mirror. Such an analysis is particularly useful for recievers which only couple a limited number of spatial modes to a detection system, such as recievers in the photon counting regime using superconducting nanowire detectors[1] or coherent recievers which rely on some type of mode sorting and phase compensation technique to collect the light into a single mode.[2]

In Section 2, we review the coherent mode decomposition for a statistically stationary (monochromatic) optical field described by a mutual coherence function or cross-spectral density. The coherent mode decomposition (or Mercer expansion[3,4]) is a form of Karhunen-Loeve expansion often used in the context of modeling propagation of partially coherent beams, as it provides a means to reduce the dimensionality of the propagation of the cross-spectral density by using some truncated finite collection of uncorrelated coherent modes.[5] In our context, we assume a pure optical mode is generated at the transmitter, and we study the coherent modes of the light arriving at the aperture of the reciever before and after compensation has been applied. In this way, the beam

*yousef.k.chahine@nasa.gov

is modeled as a partially coherent optical field obtained from an ensemble of instantaneous realizations of the turbulent atmosphere along the propagation path. As discussed below, the coherent modes represent an ideal basis with which to collect and process the received field in terms of optimizing the efficiency of a mode-limited receiver assisted only by passive optics or low-order active compensation. The coherent mode decomposition is used to derive optimal performance characteristics of a mode-limited optical receiver over a free-space channel based on the atmospheric turbulence model used to characterize the channel.

2. COHERENT MODE DECOMPOSITION AND RADIAL EQUATION FOR ISOTROPIC PARTIALLY COHERENT LIGHT

2.1 Preliminaries

In the following, we assume that the optical field arriving at the receiving aperture can be described as a statistical ensemble $\{p_i, \psi_i(x, y)\}$ where ψ_i in $L^2(\mathbb{D})$ are realizations of the (square-integrable) complex optical field truncated by a finite aperture $\mathbb{D}$ on which the fields are supported, i.e., the real part represents the electric field of a single polarization component of a monochromatic beam up to an overall phase factor $e^{i\omega t}$. We further assume that the optical fields ψ_i are normalized in $L^2(\mathbb{D})$ with probability distribution $\{p_i\}$ ($\sum p_i = 1$). The ensemble may be infinite and non-orthogonal, and can be represented in the Hilbert space $L^2(\mathbb{D})$ via an associated density operator $\hat{\rho} = \sum p_i|\psi_i\rangle\langle\psi_i|$ (here, the ket notation is used only to signify the status of an object as a vector in Hilbert space; we need not refer to an actual quantum state although an identitical density operator could be realized as describing an ensemble of single-photon Fock states). The density operator can be given a diagonal representation via the spectral theorem, i.e. there exists an orthonormal basis of eigenfunctions $|\varphi_n\rangle$ and associated real eigenvalues $\lambda_n \geq 0$ satisfying

$$\hat{\rho}|\varphi_n\rangle = \lambda_n|\varphi_n\rangle. \tag{1}$$

We henceforth label the eigenvalues in descending order $\lambda_1 \geq \lambda_2 \geq ... \geq 0$, and note that the density operator can be expressed in terms of the orthonormal basis φ_n as

$$\hat{\rho} = \sum_n \lambda_n|\varphi_n\rangle\langle\varphi_n| \tag{2}$$

with $\sum \lambda_n = \mathrm{tr}(\hat{\rho}) = 1$.

Two properties of this orthogonal decomposition shall be particularly important.[3]

(1) Any optical field in the ensemble can be represented by its coherent mode expansion

$$\psi(x, y) = \sum_n c_n\varphi_n(x, y). \tag{3}$$

Assuming the ensemble includes a random global phase $e^{i\phi}$ (uniformly distributed), the coefficients in this representation are uncorrelated complex random variables with zero mean and $\langle c_i^* c_j\rangle = \lambda_j\delta_{ij}$.

(2) The Ky Fan dominance principle[6] implies that the maximum coupling efficiency for any mode-limited system is given explicitly as the sum of the largest M eigenvalues

$$\hat{\eta}_M = \sum_{i=1}^{M} \lambda_M \tag{4}$$

and is achieved by a system which couples the first M coherent modes.

For the latter property, we assume the coherent mode decomposition is applied to the ensemble after any active compensation is applied, so that the coupling from the ensemble to the mode-limited device includes only unitary transformations and orthogonal projection onto a basis of coupled modes. With this in mind, the general analysis framework developed in this paper can be applied both to passive and active optical systems, provided an expression for the spatial covariance of the field including the residual phase error is known.

2.2 Separation of variables and radial equation for isotropic partially coherent light

Calculation of the coherent modes follows directly from the eigenvalue equation 1, which can be expanded in the form of a Fredholm integral equation

$$\int_{\mathbb{D}} d^2\vec{r}_1 \Gamma(\vec{r}_1, \vec{r}_2)\varphi_n(\vec{r}_1) = \lambda_n \varphi_n(\vec{r}_2) \tag{5}$$

with integrel kernel $\Gamma(\vec{r}_1, \vec{r}_2) = \langle \psi(\vec{r}_1)^* \psi(\vec{r}_2) \rangle$ given by the spatial covariance of the field. Numerically, the solutions can be approximated by sampling the field at a finite set of N points $\vec{r}_i$ with $i = 1, ..., N$ and solving the matrix eigenvalue problem

$$\sum_{i=1}^{N} G^i{}_j \vec{\varphi}_i = \lambda_n \vec{\varphi}_j \tag{6}$$

for the eigenvectors $\vec{\varphi}_j = \varphi(\vec{r}_j)$ of the matrix $G^i{}_j = \Gamma(\vec{r}_i, \vec{r}_j)(\Delta^2 r)_i$ defined by the covariance weighted by the discretized volume element $(\Delta^2 r)_i$.

However, for isotropic partially coherent light a direct discretization as above obscures the structure of the coherent modes. In the case of a rotationally symmetric ensemble, the coherent modes $\varphi_n(\vec{r})$ separate into radial and angular components depending on the polar coordinates (r, θ) of $\vec{r}$ in the separable form

$$\varphi_{lm}(\vec{r}) = R^l_m(r) e^{-il\theta} \tag{7}$$

determined by two integral separation constants, a radial index $m \geq 1$ and an azimuthal index l.

As the angular dependence is given entirely by the term $e^{-il\theta}$, calculation of the coherent modes reduces to a determination of the radial functions R^l_m. These are solutions to a radial equation obtained from (5) by substituting (7) and expanding in polar coordinates to obtain a one-dimensional Fredholm equation for every integer l

$$\int dr_1 K^l(r_1, r_2) R^l_m(r_1) = \lambda_{lm} R^l_m(r_2) \tag{8}$$

where the radial kernel K^l is given by

$$K^l(r_1, r_2) = r_1 \int_0^{2\pi} d\theta \Gamma(r_1, r_2, \theta) e^{-il\theta}. \tag{9}$$

Here, we have used rotational symmetry to express the covariance $\Gamma(r_1, r_2, \theta)$ as a function of the radii $r_1 = |\vec{r}_1|$, $r_2 = |\vec{r}_2|$ and angular separation $\theta = \theta_1 - \theta_2$ between $\vec{r}_1$ and $\vec{r}_2$ with respect to the origin of symmetry. Note that if Γ also exhibits symmetry under reflection, i.e. if $\Gamma(r_1, r_2, \theta) = \Gamma(r_1, r_2, -\theta)$ is an even function of the angular separation, then the radial kernel $K^l = K^{|l|}$ is real and symmetric and depends only on $|l|$. In this case, the radial functions $R^l_m = R^{|l|}_m$ are real and depend only on $|l|$.

Numerically, the coherent modes can be approximated as described in (6) with the discretization now required only on the one-dimensional radial kernels K^l and one-dimensional radial functions R^l_m. In addition to greatly reducing the size of the matrix eigenvalue problem, separating the solutions as in (7) improves the numerical accuracy of the solutions, particularly with respect to the phase in low-intensity regions of the mode.

3. COHERENT MODES FOR KOLMOGOROV OPTICAL TURBULENCE

In the following analysis, we consider a monochromatic plane wave propagating through homogeneous and isotropic turbulence exhibiting a power law phase structure function $\mathcal{D}_\phi(\vec{r}_1, \vec{r}_2) = (|\vec{r}_1 - \vec{r}_2|/a_0)^\alpha$ where a_0 describes the coherence length. Neglecting the effects of fluctuations in the log-amplitude χ on the wave structure function $\mathcal{D}(r) = \mathcal{D}_\chi(r) + \mathcal{D}_\phi(r)$, the spatial covariance of the light arriving at a finite aperture can be derived for both long-exposure (LE) and short-exposure (SE) statistics,[7,8] the latter representing the statistics with the instantaneous tilt removed (e.g., in an active feedback loop with a fast-steering mirror). In the following, we assume an annular aperture defined by an outer radius a and inner radius ϵa with obscuration ratio ϵ, and work in normalized coordinates $\vec{\rho} = \vec{r}/a$. The mutual coherence functions $\Gamma_L(\vec{\rho}_1, \vec{\rho}_2)$ and $\Gamma_S(\vec{\rho}_1, \vec{\rho}_2)$ for long-exposure and short-exposure statistics are rotationally symmetric and depend only on the normalized coherence length $\rho_c = a_0/a$, radial positions $\rho_1 = |\vec{\rho}_1|$ and $\rho_2 = |\vec{\rho}_2|$, and angular separation θ (up to an overall normalization by $1/a^2$). On the domain $\mathbb{D}$ of the annular aperture defined by $\epsilon \leq \rho_1, \rho_2 \leq 1$, they are given by[7,8]

$$\Gamma_L(\rho_1, \rho_2, \theta; \rho_c, \epsilon) = \frac{1}{\pi a^2(1-\epsilon^2)} \exp\left[-\frac{1}{2}\rho_c^{-\alpha}\rho_{12}^{\alpha}\right], \tag{10}$$

$$\Gamma_S(\rho_1, \rho_2, \theta; \rho_c, \epsilon) = \frac{1}{\pi a^2(1-\epsilon^2)} \exp\left[-\frac{1}{2}\rho_c^{-\alpha}\Big(\rho_{12}^{\alpha} + k_\epsilon \rho_{12}^2 - \mathcal{G}(\rho_1, \rho_2, \theta; \epsilon, \alpha)\Big)\right] \tag{11}$$

where $\rho_{12} = \sqrt{\rho_1^2 + \rho_2^2 - 2\rho_1\rho_2\cos\theta}$ is the normalized separation distance, k_ϵ is a constant of proportionality depending on the obscuration ratio that is associated to the mean-square tilt, and $\mathcal{G}(\rho_1, \rho_2, \theta; \epsilon, \alpha)$ is a purely geometric function related to the covariance of the tilt-phase and the total phase on an annular aperture for a power law phase structure function. These are both even functions of the angular separation θ and so the radial kernels $K_L^{|l|}$ and $K_S^{|l|}$ are symmetric and are calculated using the real-valued integrals (9)

$$K_L^{|l|}(\rho_1, \rho_2) = \frac{\rho_1}{\pi a(1-\epsilon^2)} \int_0^{2\pi} d\theta e^{-\rho_c^{-\alpha}\rho_{12}^{\alpha}/2} \cos(il\theta), \tag{12}$$

$$K_S^{|l|}(\rho_1, \rho_2) = \frac{\rho_1}{\pi a(1-\epsilon^2)} \int_0^{2\pi} d\theta e^{-\frac{1}{2}\rho_c^{-\alpha}\left(\rho_{12}^{\alpha} + k_\epsilon\rho_{12}^2 - \mathcal{G}(\rho_1, \rho_2, \theta; \epsilon, \alpha)\right)} \cos(il\theta). \tag{13}$$

3.1 Kolmogorov coherent modes in circular and annular apertures

Henceforth, we shall restrict our attention to the case of Kolmogorov optical turbulence characterized by an $\alpha = 5/3$ power law and express the coherence length in terms of the Fried parameter via $D/r_0 = 2 \cdot 6.88^{-3/5}\rho_c^{-1}$. Note that the radial kernels (12) are real, symmetric, and positive-definite on $\mathbb{D}$. As a result, the coherent modes form a complete, orthonormal basis for $L^2(\mathbb{D})$, and the radial functions are real-valued and depend only on D/r_0 and the obscuration ratio ϵ. Up to sign changes at the nodes of the radial function, the phase of each coherent mode thus reduces to an exponential $e^{-il\theta}$ describing an OAM mode with topological charge l. We shall distinguish the coherent modes with the notation KL_{lm} and KS_{lm} for long- and short-exposure Kolmogorov statistics, respectively, where l and m denote the azimuthal and radial index of the mode. Intensity distributions of the first few coherent modes for $D/r_0 = 4$ and $D/r_0 = 16$ are shown in Figure 1.

For small D/r_0, the low-order modes exhibit harder cutoffs at the aperture boundary which soften as D/r_0 increases. As D/r_0 increases, the first few modes KL_{lm} already begin to converge to a limiting mode profile for $D/r_0 \gtrsim 8$, whereas the mode profiles with tilt compensation KS_{lm} continue to evolve without an apparent limit. Figure 2 shows the radial profiles of the fundamental mode KL_{01} and KS_{01} as D/r_0 increases from 1 to 50 in unit steps. Note that the diameter of the fundamental mode KL_{01} already appears to converge to a finite limit for $D/r_0 \sim 8$, whereas the diameter of the fundamental mode KS_{01} continues to decrease even past $D/r_0 \sim 50$.

The continual decrease in the diameter of the low-order modes KS_{lm} also holds true in the presence of an obscuration, with the exception that the inner diameter of the aperture puts a lower limit on the mode field diameter causing the power to concentrate in rings around the central obscuration (Figs. 1-2). As the low-order modes correspond to those with the largest eigenvalues (Sec. 3.2), this tendency of the power in the low-order modes to concentrate near the center of the aperture is in agreement with the observation that the optimal f-number for coupling light into few-mode fibers generally decreases with increasing turbulence.[9,10]

3.2 Eigenvalue spectra with and without low-order compensation

The eigenvalues λ_{lm} and σ_{lm} associated to the coherent modes KL_{lm} and KS_{lm}, respectively, characterize the maximum coupling effiency for any mode-limited system and impart a natural ordering on the coherent modes which generally depends on D/r_0 and the obscuration ratio ϵ. The eigenvalues for the first few coherent modes are listed in Table 1.

To facilitate comparison to a typical set of modes accepted by a few-mode fiber, the modes have been ordered by the normalized cutoff frequency V_c of the corresponding modes LP_{lm} for a graded-index fiber with a parabolic

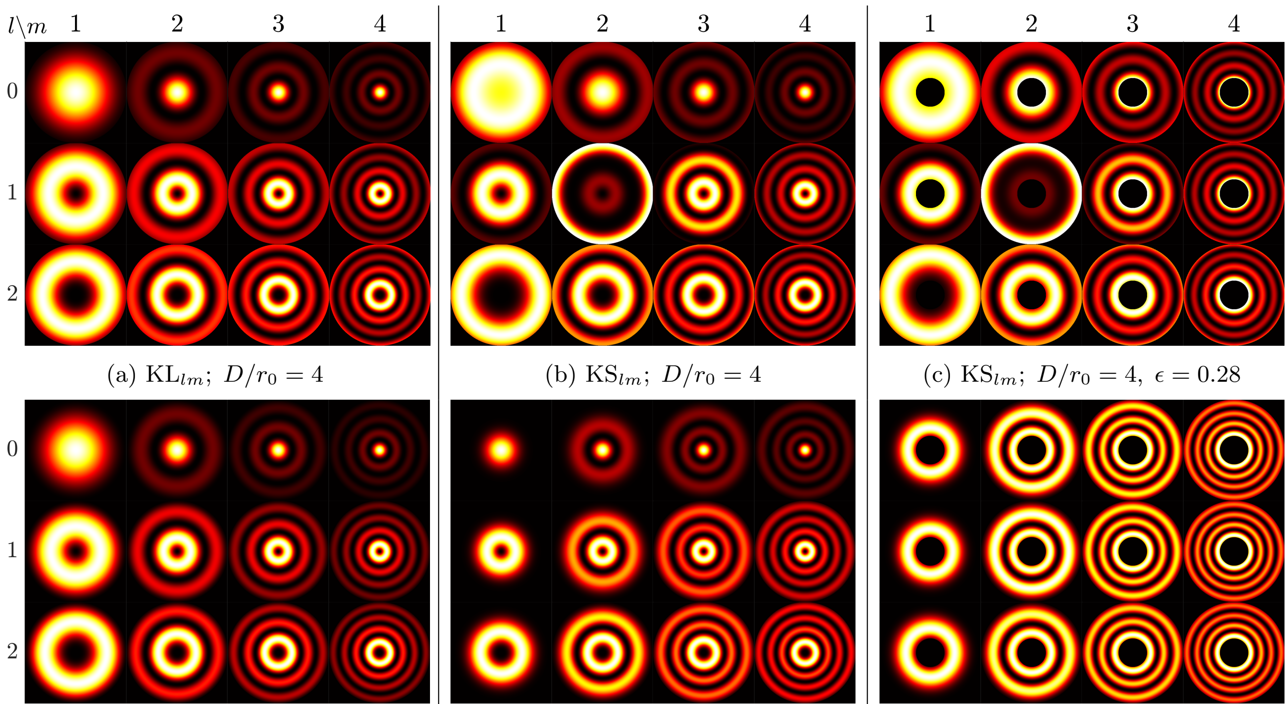

(a) $\mathrm{KL}_{lm};\ D/r_0 = 4$ (b) $\mathrm{KS}_{lm};\ D/r_0 = 4$ (c) $\mathrm{KS}_{lm};\ D/r_0 = 4,\ \epsilon = 0.28$

(d) $\mathrm{KL}_{lm};\ D/r_0 = 16$ (e) $\mathrm{KS}_{lm};\ D/r_0 = 16$ (f) $\mathrm{KS}_{lm};\ D/r_0 = 16,\ \epsilon = 0.28$

Figure 1: Intensity profiles for the first few coherent modes KL_{lm} and KS_{lm}.

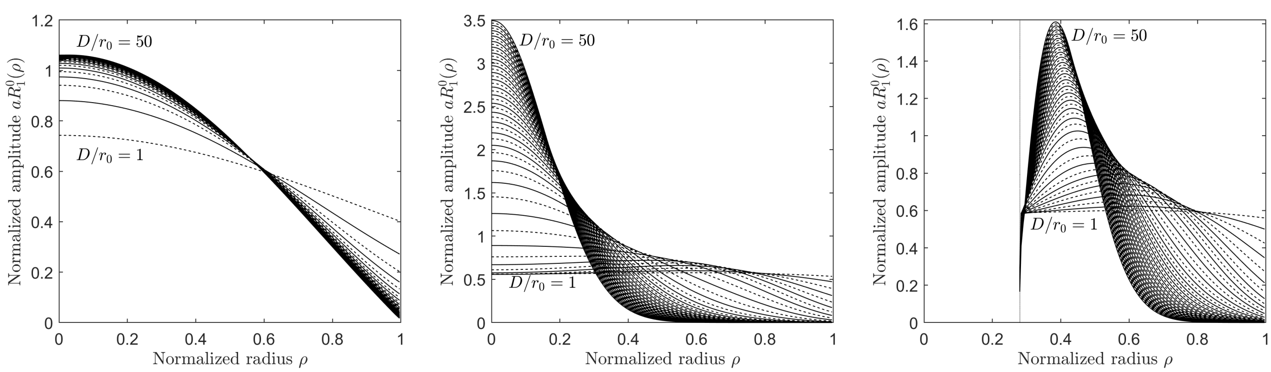

(a) KL_{01} (b) KS_{01} (c) $\mathrm{KS}_{01};\ \epsilon = 0.28$

Figure 2: Radial profile of the fundamental coherent mode with and without tilt compensation. Dashed curves are used for $D/r_0 = 1, 3, 5, ..., 49$, and solid curves are used for $D/r_0 = 2, 4, 6, ..., 50$.

profile (Sec. 4.1). For the first few coherent modes, the ordering of mode index by eigenvalue is independent of turbulence strength, but differs with and without compensation and/or obscuration. For example, with tilt compensation the $(1, 1)$ mode is demoted from the second largest eigenvalue to the fourth, behind $\mathrm{KS}_{01}, \mathrm{KS}_{02}$ and KS_{21}. Although there is some coarse similarity to the ordering of the LP modes by cutoff frequency, the precise ordering is generally different. Further investigation of the similarity of the coherent modes to the LP modes is given in Section 4.1.

3.2.1 First eigenvalue and maximum single-mode coupling efficiency

The eigenvalue of the fundamental mode describes the maximum coupling efficiency for any single-mode system. The first eigenvalue was evaluated numerically with and without tilt compensation for $D/r_0 < 1000$ and is shown

			$D/r_0 = 2$			$D/r_0 = 4$			$D/r_0 = 8$			$D/r_0 = 16$		
l	m	V_c	λ_{lm}	σ_{lm}	σ'_{lm}	λ_{lm}	σ_{lm}	σ'_{lm}	λ_{lm}	σ_{lm}	σ'_{lm}	λ_{lm}	σ_{lm}	σ'_{lm}
0	1	0.000	0.188	0.662	0.663	0.057	0.306	0.305	0.015	0.056	0.054	0.004	0.009	0.008
1	1	3.518	0.123	0.015	0.015	0.050	0.028	0.027	0.015	0.025	0.025	0.004	0.008	0.008
0	2	5.067	0.061	0.050	0.038	0.040	0.071	0.056	0.014	0.034	0.028	0.004	0.007	0.007
2	1	5.744	0.073	0.050	0.054	0.042	0.069	0.075	0.014	0.032	0.034	0.004	0.007	0.007
1	2	7.451	0.029	0.003	0.003	0.030	0.012	0.012	0.013	0.016	0.017	0.004	0.006	0.006
3	1	7.848	0.040	0.014	0.015	0.034	0.022	0.024	0.013	0.017	0.019	0.004	0.006	0.007
0	3	9.158	0.012	0.007	0.004	0.021	0.017	0.011	0.011	0.018	0.013	0.004	0.006	0.006
2	2	9.645	0.014	0.007	0.007	0.022	0.016	0.017	0.012	0.018	0.018	0.004	0.006	0.006
4	1	9.904	0.021	0.008	0.009	0.027	0.020	0.022	0.012	0.019	0.020	0.004	0.006	0.007
1	3	11.424	0.006	0.002	0.002	0.015	0.008	0.007	0.010	0.013	0.011	0.003	0.006	0.005
3	2	11.760	0.007	0.003	0.004	0.016	0.010	0.010	0.010	0.013	0.014	0.004	0.006	0.006

Table 1: Eigenvalues λ_{lm} and σ_{lm} associated to the first few coherent modes KL_{lm} and KS_{lm}, respectively. The primed columns σ'_{lm} denote the eigenvalues with obscuration $\epsilon = 0.28$. The modes are ordered by the normalized cutoff frequency V_c of the corresponding mode LP_{lm} for a graded index fiber with parabolic profile (Sec. 4.1).

in Fig. 3. The figure also shows a convenient approximation based on a fit to the numerical results given by

$$\lambda_{01} \simeq 1 - \left(\frac{(5/4)(D/r_0)^{2/3} + (8/3)(D/r_0)^2}{1 + (5/4)(D/r_0)^{2/3} + (8/3)(D/r_0)^2} \right)^{8/3}, \tag{14}$$

$$\sigma_{01} \simeq \frac{100 + 0.72(D/r_0)^{11/6}}{100 + 14.6(D/r_0)^{5/3} + 0.56(D/r_0)^{23/6}}. \tag{15}$$

This approximation for λ_{01} comes from a more general approximation for the entire spectrum as a discrete Pareto distribution (Sec. 3.2.2); a more compact approximation $\lambda_{01} \simeq (1 + (D/r_0)^{5/3})^{-6/5}$ can be made based on an approximation for the long-exposure Strehl ratio.[11]

We generally find that a relatively small obscuration does not have a significant affect on the first eigenvalue, as can be seen in Table 1 for an obscuration with $\epsilon = 0.28$. This is in contrast to the notable drop in single-mode efficiency that occurs when coupling directly to single-mode fiber due to mode mismatch with the fundamental mode LP_{01}.

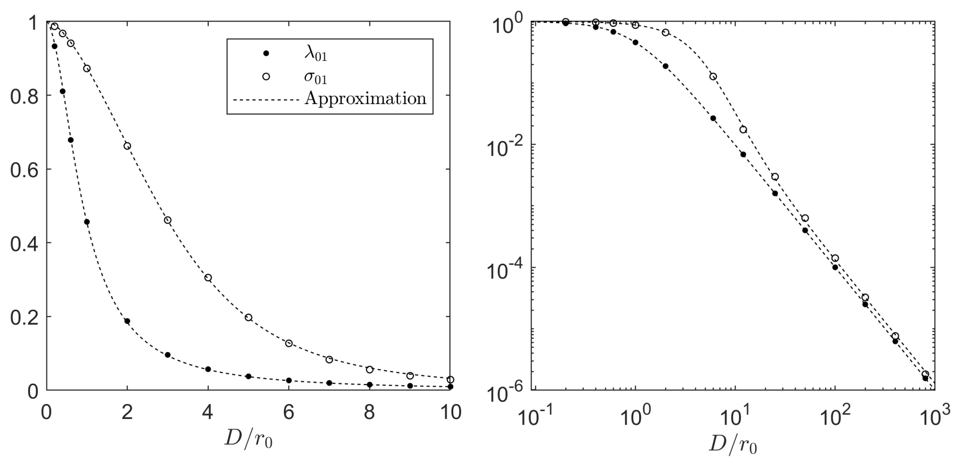

Figure 3: Largest eigenvalue for Kolmogorov optical turbulence with and without tilt compensation.

3.2.2 Power law asymptotics in the eigenvalue spectrum

Figure 4 shows the results of a numerical calculation of the first 3000 eigenvalues for $D/r_0 = 1, 2, 4, 8$, and 16 for both long- and short-exposure statistics.

In the long-exposure case, the results show that as D/r_0 increases, the spectrum transitions from a flat region containing the low-order eigenvalues to an intermediate power law region with logarithmic slope $-8/3$, and transitions again into an inverse-square power law for the higher order eigenvalues in the tail. With tilt compensation, the low-order eigenvalues exhibit a pronounced gain, and roll-off directly into an inverse-square law. The bulk of the long-exposure spectrum can be modeled with a discrete Pareto distribution $\lambda_n = P(n) - P(n-1)$ defined via discretization of the cumulative distribution function

$$P(n) = 1 - \left(\frac{N}{n+N}\right)^{\alpha} \tag{16}$$

with shape $\alpha = 8/3$ and parameter N depending on D/r_0 as $N = (5/4)(D/r_0)^{2/3} + (8/3)(D/r_0)^2$. Asymptotically this distribution underestimates the tail of the spectrum (limiting to a logarithmic slope of $-\alpha - 1 = -11/3$), but nevertheless yields a good fit for the lower order eigenvalues including 95% of the integrated spectrum.

3.2.3 Effective number of modes, purity, and von Neumann entropy

In this section, we consider the problem of determining the number of modes needed to represent a partially coherent source. One definition of the effective number of modes commonly used in this context is

$$M_{\text{eff}} = 1/\lambda_1, \tag{17}$$

or $M_{\text{eff}} = \text{tr}(\hat{\rho})/\lambda_1$ if the ensemble is not normalized.[12,13] This yields exactly the number of modes needed to represent the source in the special case that all of the non-zero eigenvalues are equal, and thus represents a minimal estimate on the number of modes needed to represent the source based only on knowledge of the relative power in the fundamental mode. More precisely, the average fidelity $\langle F \rangle_M$ of any representation of the source by a fixed set of M modes is bounded by

$$\langle F \rangle_M \leq M\lambda_1 \tag{18}$$

which reaches unity only for $M = M_{\text{eff}}$. Note that this definition can provide no general upper or lower bounds on the average fidelity of an optimal representation with M_{eff} modes beyond the trivial bound $\lambda_1 \leq \max\langle F \rangle_{M_{\text{eff}}} \leq 1$.

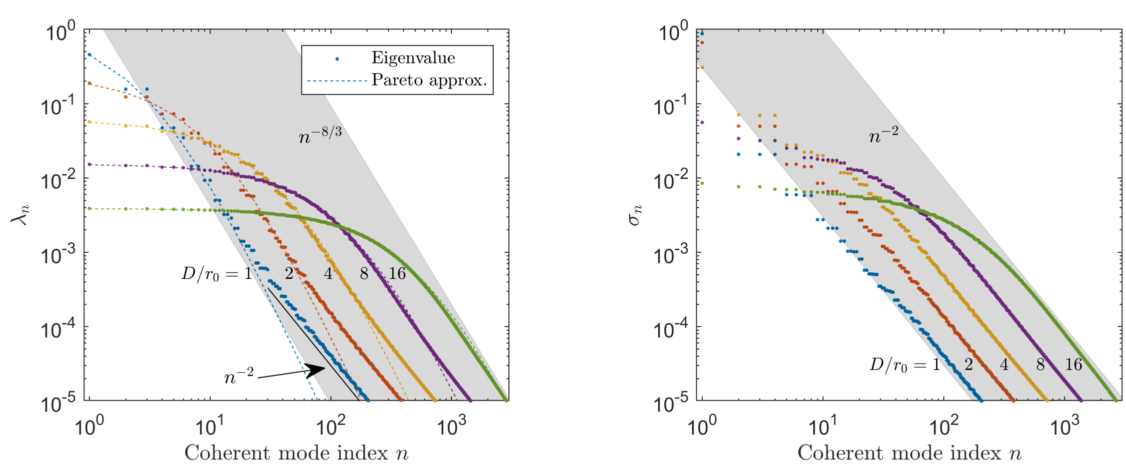

Figure 4: First 2500 coherent mode eigenvalues for Kolmogorov optical turbulence without tilt compensation (left panel) and with tilt compensation (right panel).

The results of Section 3.2.1 directly yield an approximation of M_{eff} for Kolmogorov turbulence with and without tilt-compensation.

Another measure of the effective number of modes is obtained via the reciprocal purity

$$K_{\text{eff}} = 1/\mathcal{P} = \frac{1}{\sum_{n=1}^{\infty} \lambda_n^2}. \tag{19}$$

This definition has the benefit that it can be calculated directly from the cross-spectral density or mutual coherence function without knowledge of any eigenvalues.[12] Again, this yields precisely the number of modes needed to represent the source with unit fidelity in the case that all of the non-zero eigenvalues are equal, yielding a minimal estimate based only on knowledge of the purity. However, the inequality $1/\lambda_1 \leq 1/\mathcal{P}$ implies that the purity provides a stronger estimate than is provided by knowledge of the first eigenvalue. More precisely, the average fidelity of any representation with $K \leq K_{\text{eff}}$ modes satisfies the inequality[14]

$$\langle F \rangle_K \leq \sqrt{K\mathcal{P}} \tag{20}$$

which reaches unity for $K = K_{\text{eff}}$ modes. An approximation for the purity $\mathcal{P}_L \simeq (1 + 2(D/r_0)^2)^{6/5}$ obtained from the Wigner distribution for long-exposure Kolmogorov turbulence in a circular aperture obtained in [14] was found to yield a lower bound on the average fidelity $\langle F \rangle_{K_{\text{eff}}} \sim 0.8$ for Kolmogorov turbulence.

For partially coherent sources with an infinite number of non-zero eigenvalues, the Ky Fan dominance principle implies that the error in any optimal representation with a finite number of fixed modes N is always a finite positive number given by the sum of the truncated eigenvalues. Hence, the error can only be quantified through full knowledge of the eigenvalues and becomes arbitrarily small only in the limit $N \to \infty$. Nevertheless, one can obtain a representation of such a source in a finite dimensional Hilbert space with arbitrarily small error if one allows unitary compression of a sequence of n realizations of the source using techniques from quantum information theory.[6] In this setting, the error of the representation can only be made arbitrarily small in the limit $n \to \infty$ by encoding each sequence of n "symbols" from the source in a Hilbert space with dimension at least N_{eff}^n where

$$N_{\text{eff}} = e^{S(\hat{\rho})} \tag{21}$$

and $S(\hat{\rho}) = -\sum \lambda_i \log \lambda_i$ is the von Neumann entropy of the associated density operator. In this sense, N_{eff} characterizes the minimal number of modes needed to encode the spatial mode information of the source, at least in an average sense, if one allows unitary compression of many realizations of the source.

In the context of optical propagation through turbulence, the coarse estimate provided by either the reciprocal purity $K_{\text{eff}} = 1/\sum \lambda_n^2$ or $M_{\text{eff}} = 1/\lambda_1$ is generally sufficient for practical purposes. Nevertheless, as a matter of theoretical interest, the von Neumann entropy for Kolmogorov optical turbulence with and without tilt-compensation is shown in Figure 5 for $D/r_0 \leq 15$. Fig. 5 also shows an approximation for the long-exposure

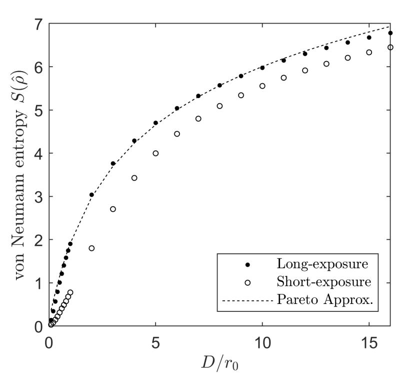

Figure 5: Von Neumann entropy of Kolmogorov optical turbulence for long- and short-exposure statistics.

entropy based on the discrete Pareto distribution model discussed in Section 3.2.2

$$S(\hat{\rho}_L) \simeq \log\left(1 + e^{11/8}[(15/32)(D/r_0)^{2/3} + (D/r_0)^2]\right) \tag{22}$$

or

$$N_{\text{eff}} \simeq 1 + e^{11/8}\big[(15/32)(D/r_0)^{2/3} + (D/r_0)^2\big]. \tag{23}$$

Note that due to the long-tailed power-law distribution of eigenvalues, the effective number of modes N_{eff} calculated via the von Neumann entropy is several times larger than the estimation based on the first eigenvalue $M_{\text{eff}} = 1/\lambda_{01} \simeq (1 + (D/r_0)^{5/3})^{6/5}$ or based on the purity $K_{\text{eff}} \simeq (1 + 2(D/r_0)^{5/3})^{6/5}$, all of which are asymptotically in proportion to the number of coherent cells within the aperture $\sim (D/r_0)^2$.

4. APPLICATIONS

In this section we consider two applications of the coherent mode decomposition presented above. First, we quantify the maximum gain one can obtain by optimal mode shaping compared to the maximum direct coupling efficiency into a graded-index few-mode fiber in the presence of turbulence. Second, we present a mode sorting technique to optimally split power equally into a finite number of modes which relies on the decorrelation of the coefficients in the coherent mode expansion.

4.1 Comparison to LP modes and maximum gain from mode shaping in turbulence

It is well-known that typical single-mode fiber modes do not provide a perfectly-matched overlap with the light from a diffraction-limited telescope, particularly in the presence of a central obscuration. In certain applications, this has motivated the development of techniques for efficient mode shaping to improve the coupling efficiency into single-mode fiber.[15,16] In the presence of turbulence with only low-order active compensation, a natural question arises as to the extent to which mode shaping can improve the coupling efficiency to few-mode fibers. In this case, one can optimize the mode shapes to match the coherent modes calculated for turbulence statistics corresponding to a targeted operating condition, and compare the resulting efficiency to that obtained by direct coupling to a typical fiber with a simple focusing system. To this end, we model coupling to a graded-index few-mode fiber with parabolic square-index profile

$$n^2(\rho) = \begin{cases} n_2^2 + (V^2/k^2)(1-\rho^2) & 0 \le \rho \le 1 \\ n_2^2 & \rho > 1 \end{cases}$$

where $\rho = r/r_c$ is the radial coordinate normalized by the core radius. The LP modes for such a fiber can be found under the weakly guiding approximation as stationary solutions of a parabolic wave equation satisfying

$$\Big(\partial_\rho^2 + \frac{1}{\rho}\partial_\rho + \frac{1}{\rho^2}\partial_\theta^2\Big)\psi + (k^2 n^2 - \beta^2)\psi = 0. \tag{24}$$

Explicitly, the modes are separable solutions of the form $\psi_{lm}(\rho,\theta) = R_l(\rho)e^{\pm il\theta}$ with radial profile

$$R_l(\rho) = \begin{cases} \rho^l e^{-V\rho^2/2} L_\nu^l(V\rho^2) & \rho \le 1 \\ K_l(V\sqrt{b_{lm}}\rho) & \rho > 1 \end{cases} \tag{25}$$

where L_ν^l is the generalized Laguerre function with $\nu = V(1-b_{lm})/4 - (l+1)/2$, K_l is the modified Bessel function of the second kind, and the normalized propagation constants b_{lm} are solutions of the characteristic equation

$$1 + 2\frac{L_{v-1}^{l+1}(V)}{L_v^l(V)} = \frac{w}{V}\frac{K_{l+1}(w)}{K_l(w)} \tag{26}$$

with $v = V\sqrt{b_{lm}}$ and $w = V\sqrt{1-(4/V)(v+(l+1)/2)}$. The solutions of the characteristic equation determine the number of radial orders $m \ge 1$ for each integer $l \ge 0$, which defines the set of guided modes LP_{lm} with normalized frequency V. The cutoff frequencies V_c for the first 11 guided modes are given in Table 1.

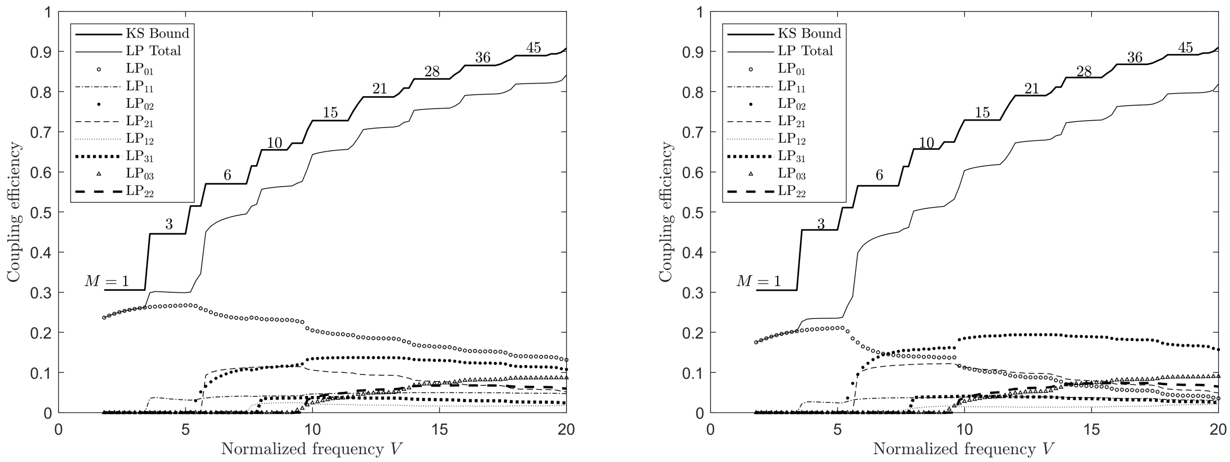

(a) $D/r_0 = 4;\ \epsilon = 0$

(b) $D/r_0 = 4;\ \epsilon = 0.28$

Figure 6: Coupling efficiency (with optimal f-number) for the LP modes of a graded-index fiber in the presence of tilt-compensated Kolmogorov turbulence with $D/r_0 = 4$, compared to the maximum coupling efficiency obtained with an equivalent number of coherent modes KS_{lm} with (a) no obscuration, and (b) obscuration ratio $\epsilon = 0.28$.

Figure 6 shows the optimal coupling efficiency calculated as the maximum value of the projected trace

$$\eta_V = \max_f \operatorname{tr}((S_f^* P_V)\hat{\rho}_S). \tag{27}$$

of the short-exposure density operator $\hat{\rho}_S$ after projection P_V onto the subspace spanned by the guided LP modes pulled back to the aperture plane by the linear canonical transformation

$$S_f = \begin{pmatrix} 0 & f \\ -1/f & 0 \end{pmatrix} \tag{28}$$

corresponding to a simple focusing system of focal length f, maximized over all f.

Note that even with moderate turbulence $D/r_0 = 4$, there is still a notable gain in coupling efficiency that can be achieved through mode-matching the coherent modes KS_{lm}, particularly in the presence of a central obscuration with obscuration ratio $\epsilon = 0.28$. The figure also shows the projections onto the one- and two-dimensional subspaces LP_{lm} for the first 8 LP modes. In particular, we note that with ideal tilt compensation, in addition to the relatively low coupling efficiency into the LP_{11} subspace resulting in poor efficiency of the 3-mode fiber, the 5th and 6th LP modes LP_{12} and LP_{31} yield relatively low coupling compared to the 7th and 8th guided modes LP_{03} and LP_{22}, resulting in a subdued gain in the transition from the 6-mode to 10-mode graded-index fiber.

4.2 An optimal method for evenly splitting power from a partially coherent source

Using the properties of the coherent mode expansion we now present a deterministic method for evenly splitting light from a partially coherent source without introducing additional losses associated to a random spatial mode diffusion process. Although this analysis is mainly concerned with the problem of evenly splitting light degraded by atmospheric turbulence, the method applies in generality to any partially coherent field. To give some context for this problem, we may consider a receiver that couples light into a finite number of discrete optical modes $\psi_1, ..., \psi_n$ which are individually coupled to an array of detectors, each with limited dynamic range (e.g. photon counting detectors using superconducting nanowires). In order to maximize the utilization of the detectors, it may be desirable to split power as evenly as possible to the available detectors. If the light has a very low degree of spatial coherence (i.e. the effective number of occupied modes is much larger than the number of modes available) the light will naturally tend to occupy all of the available modes of a typical optical system more or less evenly. However, if the spatial coherence is imposed by propagation through atmospheric turbulence, typical operating conditions may generally require coupling light which occupies fewer effective modes than are available in the receiver, often leading to larger differences in the average power going to different detectors.[17]

A number of practical solutions to this problem exist, each with its own advantages and limitations, a discussion of which we do not enter into here. Nevertheless, in this section we present a solution to this problem which may be considered optimal in the sense that it simultaneously maximizes the total coupling efficiency and minimizes the difference in average power coupled into different modes.

First, we fix the conditions with which we want to optimize the splitting ratio as specified by a given mutual coherence function $\Gamma(\vec{r}_1, \vec{r}_2)$. In order to maximize the total coupling effiiency, it follows from (4) that the system must couple the first n coherent modes, allowing only a unitary change of basis fixing this subspace. However, if the light is sorted into the coherent mode basis, the average splitting ratio realizes a worst case condition in that the maximum possible power ratio λ_1/λ_n is achieved by this basis between the first and nth coherent modes. The question then arises as to whether there exists a unitary change of basis for which the average power coupled into each mode is equal to $(\lambda_1 + \lambda_2 + ... + \lambda_n)/n$. We now construct such a basis using the decorrelation property of the coherent mode expansion (3).

The idea is to construct an orthonormal basis consisting of superpositions of the form

$$|\psi_k\rangle = \frac{1}{\sqrt{n}}\Big(e^{i\phi_1}|\varphi_1\rangle + e^{i\phi_2}|\varphi_2\rangle + ... + e^{i\phi_n}|\varphi_n\rangle\Big) \tag{29}$$

where $|\varphi_1\rangle, ..., |\varphi_n\rangle$ are the first n coherent modes. Assuming such an orthonormal basis can be found, the average coupling efficiency into such a mode is obtained using the coherent mode expansion (3) as

$$\eta_k = \frac{1}{n}\left\langle \Big|\sum_{j=1}^{\infty}\sum_{i=1}^{n} c_i e^{-i\phi_i}\langle\varphi_i|\varphi_j\rangle\Big|^2 \right\rangle = \frac{1}{n}\left\langle \Big|\sum_{i=1}^{n} c_i e^{-i\phi_i}\Big|^2 \right\rangle = \frac{1}{n}\sum_{i=1}^{n}\sum_{j=1}^{n}\langle c_i^* c_j\rangle e^{i(\phi_i-\phi_j)} = \frac{1}{n}\sum_{j=1}^{n}\lambda_j \tag{30}$$

where the last identity crucially relies on the decorrelation property of the coefficients in this expansion.

A basis of n orthogonal states $|\psi_0\rangle, ..., |\psi_{n-1}\rangle$ of the form (29) can be constructed in the form of a coherent-mode Fourier basis

$$|\psi_k\rangle = \frac{1}{\sqrt{n}}\sum_{m=1}^{n} e^{2\pi i k m/n}|\varphi_m\rangle \tag{31}$$

with $k = 0, 1, ..., n-1$. The orthogonality of this basis follows from properties of the cyclic group $\mathbb{Z}/n\mathbb{Z}$ realized as the n-th roots of unity $\omega_n = e^{2\pi i/n}$. To see this, we calculate

$$\langle\psi_j|\psi_k\rangle = \frac{1}{n}\sum_{m=0}^{n-1} e^{2\pi i m(k-j)/n} = \frac{1}{p}\sum_{m=0}^{p-1}\omega_p^m = \delta_{jk} \tag{32}$$

where we have used the fact that the exponential $e^{2\pi i(k-j)/n}$ generates a cyclic subgroup $\mathbb{Z}/p\mathbb{Z}$ of $\mathbb{Z}/n\mathbb{Z}$ of order $p = n/\gcd(n, k-j)$. The final identity then follows from the fact that the sum of the p-th roots of unity $\omega_p^0 + ... + \omega_p^{p-1} = 0$ for any integer $p > 1$ and reduces to $\omega_1^0 = 1$ for $p = 1$.

4.2.1 Optimally splitting light after propagation through turbulence

Practical implementation of the method described in the previous section requires some type of mode shaping and mode sorting technique, with the obvious limitation that the implementation loss in such a system generally increases with the number of optical elements (and hence modes) accepted by the system. Furthermore, for a passive system one must choose the turbulence conditions determining the coherent mode basis with which to optimize the system. For the latter problem, as the dependence of coupling efficiency on mode structure tends to decrease as turbulence D/r_0 increases, we propose that by optimizing the splitting using a coherent basis for moderate turbulence conditions, the reduction in coupling efficiency at higher turbulence conditions is minimal. As an example, Figure 7 shows the results of a simulation of the instantaneous power distribution at various turbulence levels for a coherent-mode Fourier basis (31) with 6 modes optimized for short-exposure statistics KS_{lm} at $D/r_0 = 4$. The simulations, performed using Kolmogorov phase screens with the Zernike tilt removed, show that although the $k = 0$ channel remains distinguished at low D/r_0 by its relatively low variance compared to the other channels, the average power in each channel remains very close to balanced from $D/r_0 = 1$ up to $D/r_0 = 8$. The question of the performance of the coherent-mode Fourier basis using Kolmogorov coherent modes in the presence of non-Kolmogorov turbulence is left for future consideration.

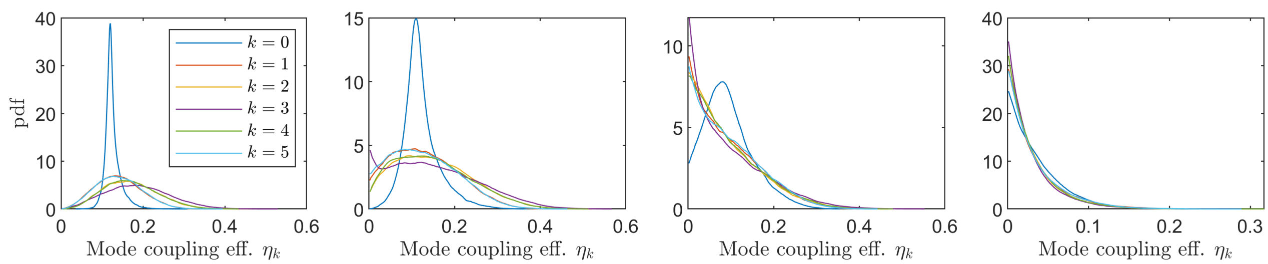

(a) $D/r_0 = 1$ (b) $D/r_0 = 2$ (c) $D/r_0 = 4$ (d) $D/r_0 = 8$

Figure 7: Simulated coupling efficiency probability density functions for a 6-mode coherent-mode Fourier basis based on short-exposure coherent modes KS_{lm} optimized at $D/r_0 = 4$.

ACKNOWLEDGMENTS

The author would like to acknowledge Brian Vyhnalek, Sarah Tedder, and Ioannis Roudas for a number of useful discussions during the development of this work. This research is supported by the NASA Space Communications and Navigation (SCaN) Program and the Glenn Research Center Communications & Intelligent Systems Division.

REFERENCES

[1] Downey, J. N., Tedder, S. A., Vyhnalek, B. E., Lantz, N. C., Marsden, M. A., Simon, W. P., Bizon, T. P., and Zeleznikar, D. J., "A real-time optical ground receiver for photon starved environments," in [*Free-Space Laser Communications XXXV*], Submitted, International Society for Optics and Photonics, SPIE (2023).

[2] Billaud, A., Orieux, A., Gomez, F., Michel, T., Bernard, S., Allioux, D., and Pinel, O., "10 Gbps free space optical communication link using Multi-Plane Light Conversion turbulence mitigation," in [*International Conference on Space Optics — ICSO 2022*], Minoglou, K., Karafolas, N., and Cugny, B., eds., **12777**, 127774R, International Society for Optics and Photonics, SPIE (2023).

[3] Mandel, L. and Wolf, E., [*Optical Coherence and Quantum Optics*], Cambridge University Press (1995).

[4] Alonso, M. A., "Wigner functions in optics: describing beams as ray bundles and pulses as particle ensembles," *Adv. Opt. Photon.* **3**, 272–365 (Dec 2011).

[5] Davis, B. J. and Schoonover, R. W., "Computationally efficient coherent-mode representations," *Optics Letters* **34**, 923 (Apr. 2009).

[6] Preskill, J., "Quantum shannon theory," (2018).

[7] Fried, D. L., "Optical resolution through a randomly inhomogeneous medium for very long and very short exposures," *J. Opt. Soc. Am.* **56**, 1372–1379 (Oct 1966).

[8] Heidbreder, G., "Image degradation with random wavefront tilt compensation," *IEEE Transactions on Antennas and Propagation* **15**(1), 90–98 (1967).

[9] Tedder, S. A., Floyd, B., Chahine, Y. K., Croop, B., Vyhnalek, B. E., Betters, C., and Leon-Saval, S. G., "Measurements of few-mode fiber photonic lanterns in emulated atmospheric conditions for a low earth orbit space to ground optical communication receiver application," in [*Free-Space Laser Communications XXXII*], Hemmati, H. and Boroson, D. M., eds., **11272**, 183 – 192, International Society for Optics and Photonics, SPIE (2020).

[10] Chahine, Y. K., Rushton, F., Vyhnalek, B. E., and Tedder, S. A., "Numerical phase space optics methods and applications to the analysis of fiber coupling efficiency in atmospheric turbulence," in [*Free-Space Laser Communications XXXIV*], Hemmati, H. and Robinson, B. S., eds., *Society of Photo-Optical Instrumentation Engineers (SPIE) Conference Series* **11993**, 119930U (Mar. 2022).

[11] Andrews, L. C. and Phillips, R. L., [*Laser Beam Propagation through Random Media*], SPIE Publications, Bellingham, Washington, 2 ed. (2005).

[12] Starikov, A., "Effective number of degrees of freedom of partially coherent sources," *J. Opt. Soc. Am.* **72**, 1538–1544 (Nov 1982).

[13] Ostrovsky, A. S., [*Coherent-mode representations in optics*], vol. PM164, SPIE, Bellingham, Washington (2006).

[14] Chahine, Y. K., Tedder, S. A., Staffa, J., and Vyhnalek, B. E., "Optimal efficiency for passively coupling partially coherent light into mode-limited optical waveguides," *J. Opt. Soc. Am. A* **38**, 1732–1743 (Dec 2021).

[15] Jovanovic, N., Schwab, C., Guyon, O., Lozi, J., Cvetojevic, N., Martinache, F., Leon-Saval, S., Norris, B., Gross, S., Doughty, D., Currie, T., and Takato, N., "Efficient injection from large telescopes into single-mode fibres: Enabling the era of ultra-precision astronomy," *A & A* **604**, A122 (2017).

[16] Gris-Sánchez, I., Ras, D. V., and Birks, T. A., "The airy fiber: an optical fiber that guides light diffracted by a circular aperture," *Optica* **3**, 270–276 (Mar 2016).

[17] Tedder, S. A., Vyhnalek, B. E., Chahine, Y. K., and Floyd, B., "Insertion loss of a multi-plane light conversion device with few mode fiber outputs under atmospheric conditions," in [*Free-Space Laser Communications XXXIV*], Hemmati, H. and Robinson, B. S., eds., **11993**, 1199305, International Society for Optics and Photonics, SPIE (2022).